

000 001 002 003 004 005 006 007 008 009 010 011 012 013 014 015 016 017 018 019 020 021 022 023 024 025 026 027 028 029 030 031 032 033 034 035 036 037 038 039 040 041 042 043 044 045 046 047 048 049 050 051 052 053 UNIAIDET: A UNIFIED AND UNIVERSAL BENCH- MARK FOR AI-GENERATED IMAGE CONTENT DETEC- TION AND LOCALIZATION

006
007 **Anonymous authors**
008 Paper under double-blind review

011 ABSTRACT

013 With the rapid proliferation of image generative models, the authenticity of digital
014 images has become a significant concern. While existing studies have proposed
015 various methods for detecting AI-generated content, current benchmarks are lim-
016 ited in their coverage of diverse generative models and image categories, often
017 overlooking end-to-end image editing and artistic images. To address these lim-
018 itations, we introduce UniAIDet, a unified and comprehensive benchmark that
019 includes both photographic and artistic images. UniAIDet covers a wide range
020 of generative models, including text-to-image, image-to-image, image inpainting,
021 image editing, and deepfake models. Using UniAIDet, we conduct a compre-
022 hensive evaluation of various detection methods and answer three key research
023 questions regarding generalization capability and the relation between detection
024 and localization. Our benchmark and analysis provide a robust foundation for
025 future research.¹

026 1 INTRODUCTION

029 Image generative models have demonstrated impressive capabilities in synthesizing realistic images
030 (Sauer et al., 2022; Betker et al., 2023; Wu et al., 2025a). However, this powerful capability raises
031 significant concerns regarding image authenticity. Malicious use cases, such as deepfakes, involve
032 passing off generated images as real to spread misinformation, or seeking improper profits by selling
033 AI-generated artworks as human-created pieces.

034 Numerous studies have been conducted to address this problem. The majority of this research,
035 however, concentrates solely on detecting entirely generated images. For instance, benchmarks like
036 GenImage (Zhu et al., 2023) and AIGCDetect (Zhong et al., 2023), as well as methods such as
037 (Chen et al., 2024a; Yan et al., 2024a; Tan et al., 2024b), are all primarily designed for binary clas-
038 sification and overlook fine-grained localization. Furthermore, they often neglect artistic content,
039 which significantly limits their generalization capabilities. ImagiNet (Boychev & Cholakov, 2025)
040 is a benchmark containing both photographic and artistic images, yet it still fails to cover partly
041 generated images and support localization task.

042 Other studies have extended this task to include localization, a critical capability for identifying
043 the generated parts within an image. Notable examples include benchmarks and methods such
044 as FakeShield (Xu et al., 2024) and SIDA (Huang et al., 2025) for photos, and DeepFakeArt
045 (Aboutalebi et al., 2023) for paintings. However, these works typically consider a very limited
046 range of generative methods (often only one or two), which significantly restricts the generaliza-
047 tion capability of their proposed benchmarks and methods. Furthermore, they universally neglect
048 a crucial and increasingly popular category of generative models: instruction-guided image editing
049 models, such as (Brooks et al., 2023).

050 With the aforementioned shortcomings in existing studies, there are several key problems lacking
051 thorough discussion, including the relation between detection and localization and the generalization

052 ¹We release a subset of our benchmark in <https://anonymous.4open.science/r/UniAIDet-46D3> since the whole benchmark is too large to be anonymously shared. We will make
053 the whole benchmark public upon acceptance.

054
 055
 056
 057
 058
 059
 060 Table 1: Examples of test images in our benchmark. T2I refers to images generated through a text-
 061 to-image model. I2I refers to images generated using image-to-image models. Edit refers to images
 062 generated using instruction guided image editing models. Inpaint refers to images generated using
 063 inpainting models. DeepFake refers to images generated using deepfake methods. For Edit, Inpaint,
 064 and DeepFake images, we label the generated parts in red.
 065
 066
 067
 068
 069
 070
 071

	Real	T2I	I2I	Edit	Inpaint	DeepFake
Photo						
Art						

072
 073
 074 capability of existing detection and localization methods, especially on partly generated images and
 075 on different categories of images.
 076

077 In this study, we introduce UniAIDet, a unified and universal benchmark for AI-generated image
 078 content detection and localization. Our benchmark encompasses a diverse range of image categories,
 079 including both photographic and artistic images (such as famous paintings and popular anime). It
 080 covers the outputs of a wide array of generative models, including text-to-image, image-to-image,
 081 image editing, image inpainting, and deepfake models. What's more, each partial generated image
 082 (e.g. inpainting, editing and deepfake) is meticulously provided with a mask that indicates the
 083 specific AI-generated regions for evaluating localization methods. Comprising a total of 80k real
 084 and generated images and covering 20 generative models, our benchmark represents the first large-
 085 scale and wide-coverage dataset for this task. Examples from our benchmark are presented in Table
 086 1.
 087

088 Using our benchmark, we conducted a comprehensive evaluation of various detection and localiza-
 089 tion methods, including those designed for detection-only and joint detection&localization models.
 090 Our results reveal that existing methods perform poorly on our benchmark, underscoring its value in
 091 exposing current limitations.
 092

093 Furthermore, we address three key research questions, including the relation between detection and
 094 localization, the generalization capability on different generative models, and the generalization
 095 capability on different categories of images. Our findings suggest that a good detection performance
 096 generally leads to good localization performance, and generalization is still a challenging problem.
 097

098 To summarize, our contributions are listed as follows:
 099

- 100 • We propose the first large-scale, wide-coverage benchmark AI-generated image content
 101 detection and localization, covering most potential practical scenarios.
 102
- 103 • We conduct a wide range of evaluation, revealing the shortcomings of previous AI-
 104 generated image detection and localization methods.
 105
- 106 • We perform deep analysis and answer three important research questions regarding general-
 107 ization and the relation between detection and localization, providing essential conclusions
 108 for future research.
 109

110 2 RELATED WORKS

111 Numerous benchmarks have been proposed to evaluate AI-generated image detectors, including
 112 widely used datasets like UniversalFakeDetect (Ojha et al., 2023), GenImage (Zhu et al., 2023),
 113

108 and AIGCDetect Zhong et al. (2023). SIDBench (Schinas & Papadopoulos, 2024) ensembles existing
 109 benchmarks to provide a larger benchmark. More recently, WildFake (Hong & Zhang, 2024),
 110 Chameleon (Yan et al., 2024a), and AIGIBench (Li et al., 2025b) were introduced to incorporate
 111 newer generative models. However, these benchmarks only support binary classification, lacking
 112 fine-grained localization capabilities and containing no artistic images, which significantly limits
 113 their application range.

114 Benchmarks designed for both AI-generated image detection and localization have also emerged.
 115 Recent studies like FakeShield (Xu et al., 2024) and SID-Set (Huang et al., 2025) focus on photos,
 116 while DeepFakeArt (Aboutalebi et al., 2023) is dedicated to artistic images. These benchmarks
 117 provide both generated images and corresponding masks that indicate the synthesized regions. How-
 118 ever, a significant limitation is their narrow coverage of generative models. Specifically, they contain
 119 very few generative models, which may lead to biased evaluation results. Furthermore, they univer-
 120 sally overlook a crucial and widely used type of generative model: instruction-guided image editing
 121 models. While LEGION (Kang et al., 2025) proposes another benchmark, its focus is on detecting
 122 artifacts rather than generated content, representing a slightly different research context.

123 Numerous detection methods have been proposed to address this problem. Early research efforts,
 124 such as those by (Wang et al., 2020) and (Liu et al., 2020), served as foundational works for detecting
 125 AI-generated images. Subsequent studies leveraged models like CLIP (Ojha et al., 2023) and its
 126 finetuned variants (Yan et al., 2024b; Tan et al., 2025; Keita et al., 2025), while other methods
 127 include DRCT (Chen et al., 2024a) and NPR (Tan et al., 2024a). Furthermore, many approaches
 128 have utilized frequency-based features to improve detection, including FreqNet (Tan et al., 2024b),
 129 AIDE (Yan et al., 2024a), and SAFE (Li et al., 2025a). There are also methods using reconstruction
 130 to train a detection model, such as DIRE (Wang et al., 2023) and FIRE (Chu et al., 2025). A
 131 significant limitation of these methods, however, is that they lack the ability to perform localization
 132 on partially generated images.

133 Some methods are designed to support both detection and localization, such as HiFi-Net (Guo et al.,
 134 2023). More recent approaches, including FakeShield (Xu et al., 2024) and SIDA (Huang et al.,
 135 2025), additionally incorporate reasoning capabilities. However, a significant limitation of these
 136 methods is their evaluation on a very restricted set of generative models and photo-only content,
 137 which makes their generalization capabilities dubious.

139 3 BENCHMARK CONSTRUCTION

140 3.1 TASK DEFINITION AND BENCHMARK OVERVIEW

141 The task of AI-generated image content detection and localization can be formalized as follows.
 142 Given an image $I \in \mathbb{R}^{C \times H \times W}$ with pixels $I_{i,j}$, a **real** image is defined as one where no pixel $I_{i,j}$ is
 143 produced by an AI generative model. Conversely, a **synthetic** image contains at least one pixel $I_{i,j}$
 144 that is AI-generated. The **detection** task is a binary classification problem to determine whether an
 145 image is real or synthetic. The **localization** task aims to identify the set of pixel positions $\{(i, j)\}$
 146 corresponding to the AI-generated regions.

147 We categorize practical AI generative models into two categories: **holistic synthesis models**, which
 148 produce a completely synthetic image, and **partial synthesis models**, which generate a partially
 149 modified image with some regions synthetic while others remain unchanged from a real image.
 150 Holistic synthesis models include text-to-image and image-to-image models (we do not discuss
 151 unconditional generative models, as they are not widely used in practice today). Partial synthesis
 152 models, on the other hand, include image inpainting, image editing, and deepfake methods.

153 It is important to note two key factors. First, unlike LEGION (Kang et al., 2025), our localization
 154 task directly focuses on whether a pixel was produced by an AI generative model, irrespective of its
 155 realism or the presence of artifacts. We argue that the core issue with generated images stems from
 156 the generative process itself, not from the lack of realism in the final output.

157 Secondly, we define purely human-created paintings and drawings as real images, as their creation
 158 process does not involve AI generative models. This definition aligns with the requirements of the
 159 community, where users often prefer works created by human artists over those generated by AI.

162 Table 2: Comparison between our proposed benchmark and existing benchmarks. ✓ refers to only
 163 containing some kind of partial synthesis model instead of all kinds of partial synthesis models.
 164

Benchmark	Content (Photo & Art)	Holistic Synthesis Model	Partial Synthesis Model	Localization	#Generative Models
DeepFakeArt	✗	✓	✓	✓	2
GenImage	✗	✓	✗	✗	8
ImagiNet	✓	✓	✗	✗	7
AIGCDetct	✗	✓	✗	✗	16
WildFake	✗	✓	✗	✗	23
Chalmeon	✗	✓	✗	✗	Unk
AIGIBench	✗	✓	✓	✗	25
FakeShield	✗	✗	✓	✓	2
SID-Set	✗	✓	✓	✓	2
UniAIDet(Ours)	✓	✓	✓	✓	20

176
 177 Table 2 provides a comprehensive comparison of our proposed benchmark with popular existing
 178 ones. Our benchmark stands out by offering a comprehensive evaluation for AI-generated image
 179 detection and localization methods, thanks to its wide coverage of image categories (photographic
 180 and artistic), diverse generative model categories, and a large number of included generative models.
 181 In contrast, other benchmarks exhibit significant limitations in one or more of these aspects, such as
 182 a lack of coverage on partial synthesis models.
 183

185 3.2 REAL IMAGES COLLECTION

187 To construct a universal benchmark, we first collected real images from multiple resources. For
 188 photographic images, we sourced real images from MSCOCO (Lin et al., 2014) and NYTimes800k
 189 (Tran et al., 2020). NYTimes800k was specifically included to enhance the diversity of our bench-
 190 mark. For artistic images, we sourced images from WikiArt (wik)² and Danbooru³. We specifically
 191 selected data created prior to 2023 to ensure the images were predominantly human-generated.

192 To ensure the quality of our benchmark, we applied an NSFW detector (Dosovitskiy et al., 2020;
 193 Falconsai, 2023) to the collected images to filter out potentially inappropriate content. These real
 194 images are collected from open-source datasets and used for research only, fully respecting their
 195 copyright.

197 3.3 SYNTHETIC IMAGES GENERATION

199 We further categorize generative models into five sub-categories, including text-to-image models
 200 and image-to-image models (which are holistic synthesis models), image inpainting models, image
 201 editing models, and deepfake methods (which are partial synthesis models). The detailed generation
 202 process for each category is presented as follows. Other details about our benchmark construction
 203 can be found in Appendix A.

205 **Text-to-Image Models** For each text-to-image model, we first source several real images and
 206 generate captions using Gemma3-4B (Team, 2025). The resulting captions are then used as prompts for
 207 the text-to-image models to generate synthetic images. We utilize 8 open-source models, includ-
 208 ing Stable-Diffusion-1.5 (Rombach et al., 2022), Stable-Diffusion-XL (Podell et al., 2023), Pixart-
 209 Sigma-XL-ms (Chen et al., 2024b), FLUX.1-Dev (Labs, 2024), Stable-Diffusion-3 (Esser et al.,
 210 2024), Stable-Diffusion-3.5-Medium (Esser et al., 2024), Stable-Diffusion-3.5-Large-Turbo (Esser
 211 et al., 2024), and Qwen-Image (Wu et al., 2025a), along with one closed-source model, SeedDream
 212 (Gao et al., 2025).

213
 214 ²<https://www.kaggle.com/datasets/ipythonx/wikiart-gangogh-creating-art-gan>

215 ³Data sourced from <https://huggingface.com/datasets/animelover/danbooru2022>,
<https://www.kaggle.com/datasets/mylesoneill/tagged-anime-illustrations>

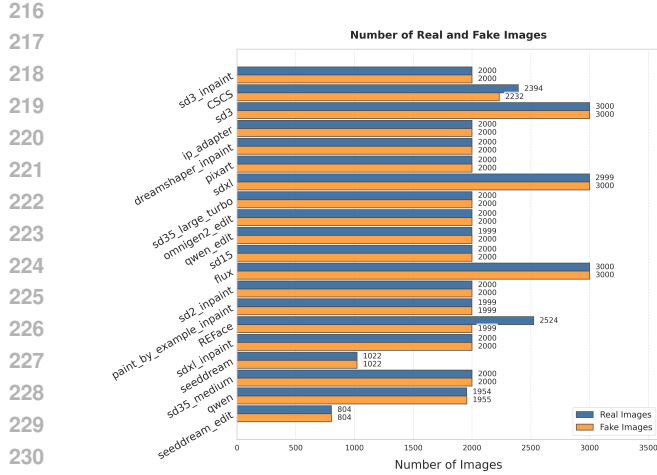


Figure 1: Data distribution of our benchmark.



Figure 2: Overview of generative models used in the benchmark.

231
232
233
234
235 **Image-to-Image Models** For each image-to-image model, we first source several real images and
236 generate captions using Gemma3-4B (Team, 2025). The resulting captions, along with the original
237 images, are then used as input to the image-to-image models to generate synthetic images. We utilize
238 one open-source model: IP-Adapter (Ye et al., 2023).

239
240 **Image Inpainting Models** For each image inpainting model, we source several real images and
241 generate masks using Segment-Anything-Model (Ravi et al., 2024). Each image is then fed into
242 the image inpainting model along with a randomly selected mask to generate partially synthetic
243 (inpainted) images. After generation, we clip the synthesized region (following the mask) from the
244 generated image and paste it back into the original image. The combined image then serves as the
245 final synthetic image. The mask is used as the ground truth of the generated region for evaluating
246 localization methods. We utilize five open-source inpainting models: SD2 Inpaint (Rombach et al.,
247 2022), SD3 Inpaint (Esser et al., 2024), SDXL Inpaint (Podell et al., 2023), DreamShaper-v8 (Lykon,
248 2023), and Paint-By-Example (Yang et al., 2023).

249
250 **Image Editing Models** For each image editing model, we source several real images and generate
251 editing instructions using Gemma3-4B (Team, 2025). We do not restrict the range of editing prompts
252 to improve the diversity of generated images. Our obtained editing prompts include add, remove,
253 modify an object, background, and style. The resulting instructions, along with the original image,
254 are then provided as input to the image editing models to generate edited images. After generating
255 the edited images, we compare each edited image with its original counterpart to identify regions
256 with notable changes as masks. We retain only the regions that are large enough, which are then
257 pasted back into the original images to create the final synthetic images. The mask of these regions
258 serve as the ground truth of the generated area for evaluating localization methods. We utilize two
259 open-source image editing models: Qwen-Image-Edit (Wu et al., 2025a) and OmniGen-2 (Wu et al.,
260 2025b), alongside one closed-source model, SeedDream-Edit (Gao et al., 2025).

261 **DeepFake Methods** We utilize the FFHQ (Karras et al., 2019) dataset as our source for facial
262 images. We then perform face swapping using faces from FFHQ on several sourced real images to
263 generate synthetic images. We use two open-source deepfake methods, REFace (Baliah et al., 2024)
264 and CSCS (Huang et al., 2024), to generate these synthetic images. The mask produced by these
265 methods is used as the ground truth of the generated regions.

3.4 BENCHMARK DETAILS

266
267 We present basic statistics of our benchmark in Figure 1 and an overview of the generative models
268 included in Figure 2. More details can be found in Appendix A.

270
271
272
273 Table 3: Main results of different methods on two splits of our benchmark. AP is not calculated for
274 non-threshold methods.
275

Method	Photo					Art				
	Acc	AP	f.Acc	r.Acc	mIoU	Acc	AP	f.Acc	r.Acc	mIoU
<i>Detection-Only</i>										
CLIP	66.12	70.15	56.26	75.96	-	62.37	65.66	59.11	65.79	-
C2P-CLIP	61.53	75.46	23.32	99.27	-	59.33	65.11	24.54	94.32	-
DeeCLIP	68.90	68.40	42.76	94.64	-	64.25	61.55	40.52	88.17	-
DIRE	50.64	49.21	1.54	98.38	-	49.98	52.90	1.43	98.55	-
FIRE	52.26	53.91	97.09	8.74	-	50.00	47.46	99.97	0.03	-
Effort	71.00	75.01	68.30	73.59	-	68.40	75.41	58.70	78.31	-
DRCT	75.13	84.47	51.84	98.02	-	71.41	77.69	59.41	83.63	-
NPR	72.51	78.72	47.51	97.04	-	71.97	80.52	46.34	97.87	-
FreqNet	67.73	72.83	62.27	73.15	-	68.06	74.66	52.48	83.86	-
AIDE	73.81	80.51	51.89	95.21	-	72.76	80.91	49.12	96.66	-
SAFE	79.89	88.44	59.83	99.51	-	79.15	85.89	59.96	98.62	-
<i>Detection & Localization</i>										
HiFi-Net	60.69	68.58	22.73	97.45	3.79	62.30	69.25	28.69	96.00	6.55
FakeShield	68.53	-	82.05	55.43	17.55	60.41	-	88.62	32.27	14.24
SIDA	60.15	-	49.75	70.50	9.99	65.04	-	39.75	90.42	8.43

288
289
290 4 EXPERIMENTS AND ANALYSIS
291292 4.1 EXPERIMENT SETUP
293294 We select a wide range of methods for evaluation and categorize them into two types: detection-only
295 methods, and detection&localization methods.296 For detection-only methods, which provide only a binary classification result indicating whether an
297 image is real or synthetic. The methods evaluated in this category are CLIP (Ojha et al., 2023), C2P-
298 CLIP (Tan et al., 2025), DeeCLIP (Keita et al., 2025), DIRE (Wang et al., 2023), FIRE (Chu et al.,
299 2025), Effort (Yan et al., 2024c), DRCT (Chen et al., 2024a), NPR (Tan et al., 2024a), FreqNet (Tan
300 et al., 2024b), AIDE (Yan et al., 2024a), and SAFE (Li et al., 2025a). For DeeCLIP, Effort, DRCT,
301 C2P-CLIP, DIRE, and FIRE, we utilized the pretrained checkpoints from their original papers. For
302 the remaining methods, we use checkpoints open-sourced by (Li et al., 2025b).303 We further include three detection&localization methods, which support both detection and local-
304 ization tasks, to evaluate both their detection and localization performance. These methods are
305 HiFi-Net (Guo et al., 2023), FakeShield (Xu et al., 2024), and SIDA (Huang et al., 2025). For all of
306 these methods, we utilized their publicly released pretrained checkpoints.307 For evaluation metrics, we adopt the widely used accuracy (Acc) and average precision (AP). Fol-
308 lowing (Li et al., 2025b), we also report f.Acc (the accuracy of detecting synthetic images) and r.Acc
309 (the accuracy of detecting real images) to provide a more detailed insight into model performance.
310 For the localization task, we use mean Intersection over Union (mIoU) as the primary metric. Details
311 about our experiment setup can be found in Appendix B.
312313 4.2 RESULTS AND ANALYSIS
314315 4.2.1 OVERALL RESULTS
316317 We first report the overall results in Table 3. Several key observations can be drawn from the results.
318 First, SAFE outperformed previous methods on the detection task, demonstrating its superiority.
319 Conversely, joint detection&localization methods performed poorly on the detection task. Interest-
320 ingly, reconstruction-based methods (DIRE, FIRE) perform extremely poorly, indicating their severe
321 bias during training, an observation similar to that in Cazenavette et al. (2024).322 Regarding overall generalization, CLIP-based methods (e.g., DeeCLIP) and DRCT exhibit a notable
323 performance drop on the Art split. This indicates that the CLIP backbone may not generalize well
to detecting images of different content, which highlights a key shortcoming of several previous

324 methods and raises concerns about directly applying them to artistic images. In contrast, frequency-
 325 based methods demonstrate fine generalization ability on artistic images, suggesting that frequency-
 326 is indeed a crucial factor in identifying synthetic images, especially when used judiciously (e.g., in
 327 AIDE and SAFE).

328 The specifically trained detection&localization methods show disappointing performance on both
 329 tasks. Furthermore, these methods exhibited a significant bias towards making specific types of
 330 errors. For example, HiFi-Net and SIDA tended to misclassify synthetic images as real, while
 331 FakeShield tended to misclassify real images as synthetic. This suggests a potential robustness
 332 problem with these methods.

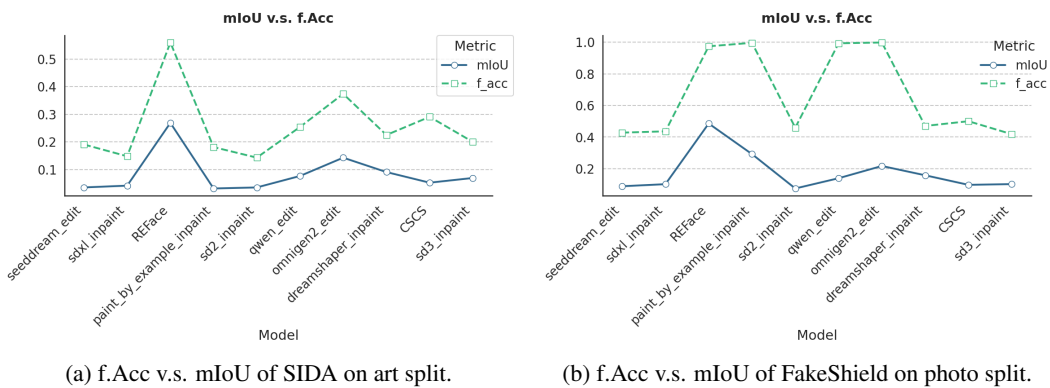
333 In summary, our findings highlight a crucial observation: current methods for AI-generated im-
 334 age detection and localization are far from mature and require significant future development. We
 335 provide more detailed discussions in Appendix C.

337 4.2.2 DETECTION V.S. LOCALIZATION

339 Given the existence of detection and localization tasks and the poor performance of detec-
 340 tion&localization methods on both, it is natural to ask whether a method’s performance trend is
 341 similar for both detection and localization tasks, which is **RQ1: Do existing methods perform**
 342 **consistently on detection and localization tasks?**

343 An observation from Table 3 is that strong detection and localization performance do not necessarily
 344 align. For example, SIDA achieves a higher detection accuracy on the Art split compared to the
 345 Photo split, yet its localization performance declines on the same split. This seems to suggest that
 346 the two tasks can sometimes be at odds with each other.

347 However, overall detection accuracy is influenced by holistic synthesis models, which may yield
 348 noisy results. To delve deeper, we present the f.Acc and mIoU for each partial synthesis model in
 349 Figure 3.



362 (a) f.Acc v.s. mIoU of SIDA on art split. (b) f.Acc v.s. mIoU of FakeShield on photo split.

363

364 Figure 3: Trends of corresponding f.Acc and mIoU.

365

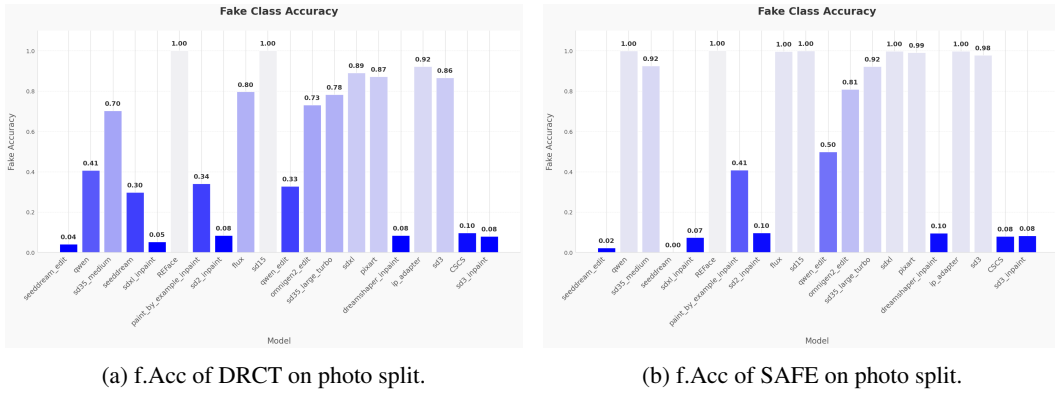
366 A clear observation is that f.Acc and mIoU exhibit nearly identical trends across both methods! This
 367 reveals that detection and localization generally do not conflict with each other. Instead, a good
 368 localization result generally correlates with a good detection result, highlighting the importance of
 369 jointly considering both tasks rather than focusing on only one.

370 **Takeaway** For detection&localization methods, they perform consistently on detection and local-
 371 ization tasks. Detection and localization do not conflict with each other.

374 4.2.3 GENERALIZATION ACROSS DIFFERENT GENERATIVE MODELS

375 Given the rapid emergence of new generative models and the varied categories of generative models,
 376 it is essential for a detection method to generalize well across different generative models, which is
 377 **RQ2: Do existing methods generalize well across different generative methods?**

378 While we have established that the overall performance of existing models is unsatisfactory—evidenced by their low average accuracy (especially f.Acc) and mIoU—we now investigate
 379 the source of this poor performance. Specifically, we aim to determine if it stems from a fundamental
 380 lack of overall capability (uniform poor performance across all generative methods) or from a
 381 lack of generalization capability (excellent performance on some generative methods but extremely
 382 poor performance on others). For detection methods, we present the f.Acc of DRCT and SAFE (two
 383 strong detectors as indicated in Table 3) in Figure 4.



(a) f.Acc of DRCT on photo split.

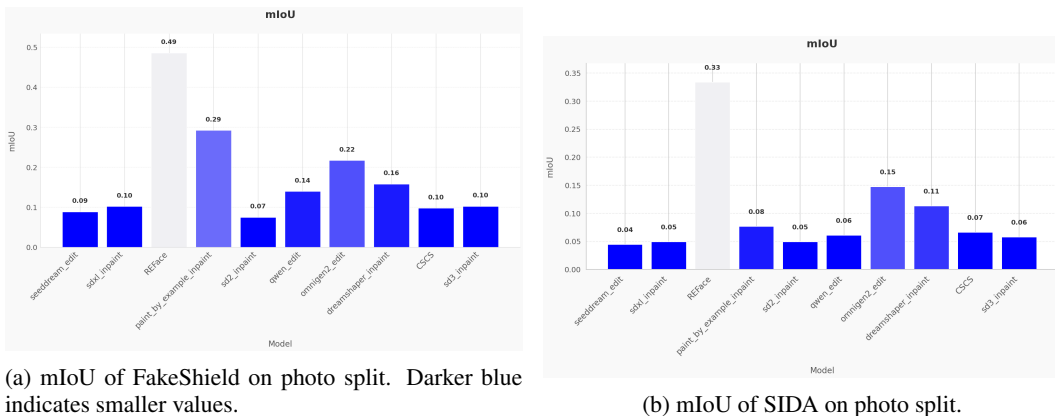
(b) f.Acc of SAFE on photo split.

Figure 4: f.Acc of different methods. Darker blue indicates smaller values.

401 Both methods perform poorly due to a lack of generalization capability. They exhibit excellent
 402 performance on certain generative models but fail significantly on others. Specifically, they fail on
 403 most partial synthesis models while performing well on most holistic synthesis models, indicating
 404 that partially generated images represent an overlooked challenge for existing detection methods.

405 Even for holistic synthesis models, both methods showed almost no effect on SeedDream, a newly
 406 released closed-source model. This highlights that, given the rapid development of generative mod-
 407 els, generalization capability remains a huge problem for synthetic image detection methods.

408 We would also like to note that these methods do not completely fail to generalize. For example, both
 409 methods perform quite well on REFace (a partial generative method) and Qwen-Image (a recently
 410 released and powerful holistic synthesis model), indicating some potential for generalization.



(a) mIoU of FakeShield on photo split. Darker blue indicates smaller values.

(b) mIoU of SIDA on photo split.

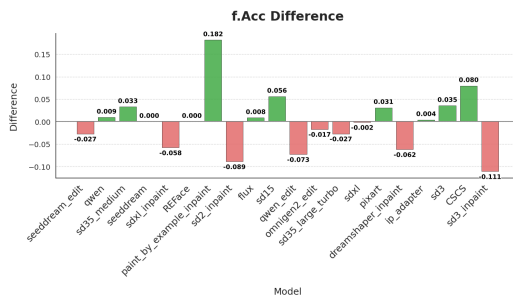
Figure 5: mIoU of different methods. Darker blue indicates smaller values.

428 We then discuss the generalization of localization methods and focus on mIoU. The results are shown
 429 in Figure 5, which shows both methods performing poorly on nearly all partial synthesis models.
 430 This indicates that the failure of localization methods does not stem from a lack of generalization, but
 431 rather from a fundamental lack of overall capability. We present a case study for this circumstance
 in Appendix C.

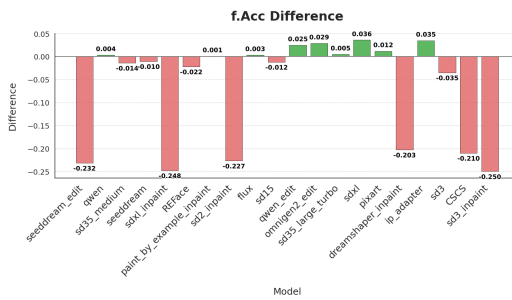
432 **Takeaway** Existing detection-only methods perform poorly on partial synthesis models, highlighting a significant issue with their generalization capability. Conversely, existing detection&localization methods perform poorly across nearly all models tested, suggesting a fundamental lack of overall capability.

437 4.2.4 GENERALIZATION ACROSS DIFFERENT CATEGORIES OF IMAGES

439 A robust method should perform consistently across different categories of images, including both
 440 photographic and artistic images. If it doesn't, its application in real-world scenarios could be prob-
 441 lematic. For example, a method proven effective on photos but not on artistic images cannot be
 442 used to determine if a drawing was created by a human artist, leading to practical difficulties. This
 443 observation leads to our **RQ3: Do existing methods generalize well across different categories**
 444 **of images?**



455 (a) Difference of f.Acc of SAFE between art split and
 456 photo split.



455 (b) Difference of f.Acc of FakeShield between art split
 456 and photo split.

458 Figure 6: The performance difference between art and photo split (art-photo). Red indicates values
 459 less than 0 while green indicates values larger than 0.

461 We calculate the difference in f.Acc for corresponding generative methods between the photo and
 462 art splits on both SAFE and FakeShield, and the results are presented in Figure 6. The results show
 463 that both methods have a performance difference between the art and photo splits. This difference
 464 is generally minimal for SAFE, with most being under 5%. However, FakeShield shows a severe
 465 performance degradation on many generative methods in the art split, which indicates a critical
 466 failure in image category generalization.

467 There is an interesting fact that both SAFE and FakeShield show a larger performance difference
 468 on partial synthesis models. Specifically, both methods tend to show performance degradation on
 469 partial synthesis models in the art split. This indicates that the generalization problem on partial
 470 synthesis models is even more severe in the art split, further revealing a generalization problem.

472 **Takeaway** Existing methods show performance differences between different kinds of image cat-
 473 egories, with more notable differences on partial synthesis models, indicating a problem in general-
 474 ization across contents.

477 5 CONCLUSION

479 This paper presents UniAIDet, a unified and universal benchmark for AI-generated image content
 480 detection and localization. Our benchmark offers comprehensive coverage of diverse image cat-
 481 egories and generative model types, and includes a large number of generative models, making it a
 482 more robust and useful source for evaluation compared to previous benchmarks with limited scope.
 483 We conduct a comprehensive evaluation of a wide range of existing methods using UniAIDet and
 484 reveal failures in existing methods. We also answer three key research questions regarding the
 485 relation between detection and localization, model generalization, and image category generalization.
 Overall, our study provides a valuable resource and highlights clear directions for future research.

486 ETHICS STATEMENT
487488 We adhere to the ICLR Code of Ethics. Our released dataset sources real images from open-source
489 datasets as indicated, following their license and copyright restrictions. Our released dataset con-
490 taining synthetic images is for research only and does not aim at conveying any information about
491 real-life.
492493 REPRODUCIBILITY STATEMENT
494495 We submit a subset of our dataset through an anonymous GitHub repo to provide an intuitive view
496 of our benchmark. The whole benchmark is too large to be gracefully hosted anonymously, and
497 we will release the whole benchmark upon acceptance. We have disclosed the models and prompts
498 used for generating synthetic images in Section 3.3 and Appendix A. We have also clearly cited the
499 detection and localization methods and discussed the checkpoints used for evaluation in Section 4.1
500 and Appendix B.
501502 REFERENCES
503504 Gangogh training data set. URL <https://github.com/rkjones4/GANGogh>.
505506 Hossein Aboutalebi, Dayou Mao, Rongqi Fan, Carol Xu, Chris He, and Alexander Wong. Deep-
507 fakeart challenge: A benchmark dataset for generative ai art forgery and data poisoning detection.
508 *arXiv preprint arXiv:2306.01272*, 2023.509 Sanoojan Baliah, Qinliang Lin, Shengcui Liao, Xiaodan Liang, and Muhammad Haris Khan. Re-
510 alistic and efficient face swapping: A unified approach with diffusion models. *arXiv preprint*
511 *arXiv:2409.07269*, 2024.513 James Betker, Gabriel Goh, Li Jing, Tim Brooks, Jianfeng Wang, Linjie Li, Long Ouyang, Juntang
514 Zhuang, Joyce Lee, Yufei Guo, et al. Improving image generation with better captions. *Computer*
515 *Science*. <https://cdn.openai.com/papers/dall-e-3.pdf>, 2(3):8, 2023.516 Delyan Boychev and Radostin Cholakov. Imagenet: A multi-content benchmark for synthetic image
517 detection, 2025. URL <https://arxiv.org/abs/2407.20020>.519 Tim Brooks, Aleksander Holynski, and Alexei A Efros. Instructpix2pix: Learning to follow image
520 editing instructions. In *Proceedings of the IEEE/CVF conference on computer vision and pattern*
521 *recognition*, pp. 18392–18402, 2023.523 George Cazenavette, Avneesh Sud, Thomas Leung, and Ben Usman. Fakeinversion: Learning to
524 detect images from unseen text-to-image models by inverting stable diffusion. In *Proceedings*
525 *of the IEEE/CVF Conference on Computer Vision and Pattern Recognition (CVPR)*, pp. 10759–
526 10769, June 2024.527 Baoying Chen, Jishen Zeng, Jianquan Yang, and Rui Yang. DRCT: Diffusion reconstruction con-
528 trastive training towards universal detection of diffusion generated images. In Ruslan Salakhut-
529 dinov, Zico Kolter, Katherine Heller, Adrian Weller, Nuria Oliver, Jonathan Scarlett, and Felix
530 Berkenkamp (eds.), *Proceedings of the 41st International Conference on Machine Learning*, vol-
531 *ume 235 of Proceedings of Machine Learning Research*, pp. 7621–7639. PMLR, 21–27 Jul 2024a.
532 URL <https://proceedings.mlr.press/v235/chen24ay.html>.533 Junsong Chen, Chongjian Ge, Enze Xie, Yue Wu, Lewei Yao, Xiaozhe Ren, Zhong-
534 dao Wang, Ping Luo, Huchuan Lu, and Zhenguo Li. Pixart- σ : Weak – to –
535 strong training of diffusion transformer for 4k text – to – image generation, 2024b.537 Beilin Chu, Xuan Xu, Xin Wang, Yufei Zhang, Weike You, and Linna Zhou. Fire: Robust detection
538 of diffusion-generated images via frequency-guided reconstruction error. In *Proceedings of the*
539 *IEEE/CVF Conference on Computer Vision and Pattern Recognition (CVPR)*, pp. 12830–12839,
June 2025.

540 Alexey Dosovitskiy, Lucas Beyer, Alexander Kolesnikov, Dirk Weissenborn, Xiaohua Zhai, Thomas
 541 Unterthiner, Mostafa Dehghani, Matthias Minderer, Georg Heigold, Sylvain Gelly, et al. An image is
 542 worth 16x16 words: Transformers for image recognition at scale. *arXiv preprint arXiv:2010.11929*,
 543 2020.

544 Patrick Esser, Sumith Kulal, Andreas Blattmann, Rahim Entezari, Jonas Müller, Harry Saini, Yam
 545 Levi, Dominik Lorenz, Axel Sauer, Frederic Boesel, et al. Scaling rectified flow transformers
 546 for high-resolution image synthesis. In *Forty-first International Conference on Machine Learning*,
 547 2024.

548 Falconsai. Fine-tuned vision transformer (vit) for nsfw image classification, 2023. URL https://huggingface.co/Falconsai/nsfw_image_detection.

549 Yu Gao, Lixue Gong, Qiushan Guo, Xiaoxia Hou, Zhichao Lai, Fanshi Li, Liang Li, Xiaochen Lian,
 550 Chao Liao, Liyang Liu, et al. Seedream 3.0 technical report. *arXiv preprint arXiv:2504.11346*,
 551 2025.

552 Xiao Guo, Xiaohong Liu, Zhiyuan Ren, Steven Grosz, Iacopo Masi, and Xiaoming Liu. Hierarchical
 553 fine-grained image forgery detection and localization. In *Proceedings of the IEEE/CVF conference*
 554 *on computer vision and pattern recognition*, pp. 3155–3165, 2023.

555 Yan Hong and Jianfu Zhang. Wildfake: A large-scale challenging dataset for ai-generated images
 556 detection, 2024. URL <https://arxiv.org/abs/2402.11843>.

557 Zhenglin Huang, Jinwei Hu, Xiangtai Li, Yiwei He, Xingyu Zhao, Bei Peng, Baoyuan Wu, Xiaowei
 558 Huang, and Guangliang Cheng. Sida: Social media image deepfake detection, localization and ex-
 559 planation with large multimodal model. In *Proceedings of the Computer Vision and Pattern Recog-*
 560 *nition Conference*, pp. 28831–28841, 2025.

561 Ziyao Huang, Fan Tang, Yong Zhang, Juan Cao, Chengyu Li, Sheng Tang, Jintao Li, and Tong-Yee
 562 Lee. Identity-preserving face swapping via dual surrogate generative models. *ACM Transactions on*
 563 *Graphics*, 43(5):1–19, 2024.

564 Hengrui Kang, Siwei Wen, Zichen Wen, Junyan Ye, Weijia Li, Peilin Feng, Baichuan Zhou, Bin
 565 Wang, Dahua Lin, Linfeng Zhang, et al. Legion: Learning to ground and explain for synthetic
 566 image detection. *arXiv preprint arXiv:2503.15264*, 2025.

567 Tero Karras, Samuli Laine, and Timo Aila. A style-based generator architecture for generative ad-
 568 versarial networks. In *Proceedings of the IEEE/CVF conference on computer vision and pattern*
 569 *recognition*, pp. 4401–4410, 2019.

570 Mamadou Keita, Wassim Hamidouche, Hessen Bougueffa Eutamene, Abdelmalik Taleb-Ahmed, and
 571 Abdenour Hadid. Deeclip: A robust and generalizable transformer-based framework for detecting
 572 ai-generated images. *arXiv preprint arXiv:2504.19876*, 2025.

573 Black Forest Labs. Flux. <https://github.com/black-forest-labs/flux>, 2024.

574 Ouxiang Li, Jiayin Cai, Yanbin Hao, Xiaolong Jiang, Yao Hu, and Fuli Feng. Improving synthetic
 575 image detection towards generalization: An image transformation perspective. In *Proceedings of*
 576 *the 31st ACM SIGKDD Conference on Knowledge Discovery and Data Mining V. 1*, pp. 2405–2414,
 577 2025a.

578 Ziqiang Li, Jiazen Yan, Ziwen He, Kai Zeng, Weiwei Jiang, Lizhi Xiong, and Zhangjie Fu. Is artificial
 579 intelligence generated image detection a solved problem? *arXiv preprint arXiv:2505.12335*, 2025b.

580 Tsung-Yi Lin, Michael Maire, Serge Belongie, James Hays, Pietro Perona, Deva Ramanan, Piotr
 581 Dollár, and C Lawrence Zitnick. Microsoft coco: Common objects in context. In *European confer-*
 582 *ence on computer vision*, pp. 740–755. Springer, 2014.

583 Zhenghe Liu, Xiaojuan Qi, and Philip HS Torr. Global texture enhancement for fake face detection in
 584 the wild. In *Proceedings of the IEEE/CVF conference on computer vision and pattern recognition*,
 585 pp. 8060–8069, 2020.

594 Lykon. Dreamshaper-v8, 2023. URL <https://huggingface.co/Lykon/dreamshaper-8-inpainting>.

595

596

597 Utkarsh Ojha, Yuheng Li, and Yong Jae Lee. Towards universal fake image detectors that generalize
598 across generative models. In *Proceedings of the IEEE/CVF Conference on Computer Vision and*
599 *Pattern Recognition*, pp. 24480–24489, 2023.

600 Dustin Podell, Zion English, Kyle Lacey, Andreas Blattmann, Tim Dockhorn, Jonas Müller, Joe Penna,
601 and Robin Rombach. Sdxl: Improving latent diffusion models for high-resolution image synthesis.
602 *arXiv preprint arXiv:2307.01952*, 2023.

603

604 Nikhila Ravi, Valentin Gabeur, Yuan-Ting Hu, Ronghang Hu, Chaitanya Ryali, Tengyu Ma, Haitham
605 Khedr, Roman Rädle, Chloe Rolland, Laura Gustafson, Eric Mintun, Junting Pan, Kalyan Vasudev
606 Alwala, Nicolas Carion, Chao-Yuan Wu, Ross Girshick, Piotr Dollár, and Christoph Feichtenhofer.
607 Sam 2: Segment anything in images and videos. *arXiv preprint arXiv:2408.00714*, 2024. URL
608 <https://arxiv.org/abs/2408.00714>.

609 Robin Rombach, Andreas Blattmann, Dominik Lorenz, Patrick Esser, and Björn Ommer. High-
610 resolution image synthesis with latent diffusion models. In *Proceedings of the IEEE/CVF Conference on Computer Vision and Pattern Recognition (CVPR)*, pp. 10684–10695, June 2022.

611

612 Axel Sauer, Katja Schwarz, and Andreas Geiger. Stylegan-xl: Scaling stylegan to large diverse
613 datasets. In *ACM SIGGRAPH 2022 conference proceedings*, pp. 1–10, 2022.

614

615 Manos Schinas and Symeon Papadopoulos. Sidbench: A python framework for reliably assessing
616 synthetic image detection methods, 2024. URL <https://arxiv.org/abs/2404.18552>.

617

618 Chuangchuang Tan, Yao Zhao, Shikui Wei, Guanghua Gu, Ping Liu, and Yunchao Wei. Rethinking the
619 up-sampling operations in cnn-based generative network for generalizable deepfake detection. In
620 *Proceedings of the IEEE/CVF Conference on Computer Vision and Pattern Recognition*, pp. 28130–
621 28139, 2024a.

622 Chuangchuang Tan, Yao Zhao, Shikui Wei, Guanghua Gu, Ping Liu, and Yunchao Wei. Frequency-
623 aware deepfake detection: Improving generalizability through frequency space domain learning. In
624 *Proceedings of the AAAI Conference on Artificial Intelligence*, volume 38, pp. 5052–5060, 2024b.

625

626 Chuangchuang Tan, Renshuai Tao, Huan Liu, Guanghua Gu, Baoyuan Wu, Yao Zhao, and Yunchao
627 Wei. C2p-clip: Injecting category common prompt in clip to enhance generalization in deepfake
628 detection. In *Proceedings of the AAAI Conference on Artificial Intelligence*, volume 39, pp. 7184–
629 7192, 2025.

630 Gemma Team. Gemma 3. 2025. URL <https://goo.gle/Gemma3Report>.

631

632 Alasdair Tran, Alexander Mathews, and Lexing Xie. Transform and tell: Entity-aware news image
633 captioning. In *Proceedings of the IEEE/CVF conference on computer vision and pattern recognition*,
634 pp. 13035–13045, 2020.

635 Sheng-Yu Wang, Oliver Wang, Richard Zhang, Andrew Owens, and Alexei A Efros. Cnn-generated
636 images are surprisingly easy to spot... for now. In *Proceedings of the IEEE/CVF conference on*
637 *computer vision and pattern recognition*, pp. 8695–8704, 2020.

638

639 Zhendong Wang, Jianmin Bao, Wengang Zhou, Weilun Wang, Hezhen Hu, Hong Chen, and Houqiang
640 Li. Dire for diffusion-generated image detection. In *Proceedings of the IEEE/CVF International*
641 *Conference on Computer Vision*, pp. 22445–22455, 2023.

642 Chenfei Wu, Jiahao Li, Jingren Zhou, Junyang Lin, Kaiyuan Gao, Kun Yan, Sheng ming Yin, Shuai
643 Bai, Xiao Xu, Yilei Chen, Yuxiang Chen, Zecheng Tang, Zekai Zhang, Zhengyi Wang, An Yang,
644 Bowen Yu, Chen Cheng, Dayiheng Liu, Deqing Li, Hang Zhang, Hao Meng, Hu Wei, Jingyuan Ni,
645 Kai Chen, Kuan Cao, Liang Peng, Lin Qu, Minggang Wu, Peng Wang, Shuting Yu, Tingkun Wen,
646 Wensen Feng, Xiaoxiao Xu, Yi Wang, Yichang Zhang, Yongqiang Zhu, Yujia Wu, Yuxuan Cai, and
647 Zenan Liu. Qwen-image technical report, 2025a. URL <https://arxiv.org/abs/2508.02324>.

648 Chenyuan Wu, Pengfei Zheng, Ruiran Yan, Shitao Xiao, Xin Luo, Yueze Wang, Wanli Li, Xiyan
 649 Jiang, Yexin Liu, Junjie Zhou, Ze Liu, Ziyi Xia, Chaofan Li, Haoge Deng, Jiahao Wang, Kun Luo,
 650 Bo Zhang, Defu Lian, Xinlong Wang, Zhongyuan Wang, Tiejun Huang, and Zheng Liu. Omnigen2:
 651 Exploration to advanced multimodal generation. *arXiv preprint arXiv:2506.18871*, 2025b.
 652

653 Zhipei Xu, Xuanyu Zhang, Runyi Li, Zecheng Tang, Qing Huang, and Jian Zhang. Fakeshield: Ex-
 654 plainable image forgery detection and localization via multi-modal large language models. *arXiv*
 655 *preprint arXiv:2410.02761*, 2024.

656 Shilin Yan, Ouxiang Li, Jiayin Cai, Yanbin Hao, Xiaolong Jiang, Yao Hu, and Weidi Xie. A sanity
 657 check for ai-generated image detection. *arXiv preprint arXiv:2406.19435*, 2024a.

658 Zhiyuan Yan, Jiangming Wang, Peng Jin, Ke-Yue Zhang, Chengchun Liu, Shen Chen, Taiping Yao,
 659 Shouhong Ding, Baoyuan Wu, and Li Yuan. Orthogonal subspace decomposition for generalizable
 660 ai-generated image detection. *arXiv preprint arXiv:2411.15633*, 2024b.
 661

662 Zhiyuan Yan, Jiangming Wang, Zhendong Wang, Peng Jin, Ke-Yue Zhang, Shen Chen, Taiping Yao,
 663 Shouhong Ding, Baoyuan Wu, and Li Yuan. Effort: Efficient orthogonal modeling for generalizable
 664 ai-generated image detection. *arXiv preprint arXiv:2411.15633*, 2024c.
 665

666 Binxin Yang, Shuyang Gu, Bo Zhang, Ting Zhang, Xuejin Chen, Xiaoyan Sun, Dong Chen, and Fang
 667 Wen. Paint by example: Exemplar-based image editing with diffusion models. In *Proceedings of*
 668 *the IEEE/CVF conference on computer vision and pattern recognition*, pp. 18381–18391, 2023.

669 Hu Ye, Jun Zhang, Sibo Liu, Xiao Han, and Wei Yang. Ip-adapter: Text compatible image prompt
 670 adapter for text-to-image diffusion models. 2023.

671 Nan Zhong, Yiran Xu, Zhenxing Qian, and Xinpeng Zhang. Rich and poor texture contrast: A simple
 672 yet effective approach for ai-generated image detection. *CoRR*, 2023.

673 Mingjian Zhu, Hanting Chen, Qiangyu Yan, Xudong Huang, Guanyu Lin, Wei Li, Zhijun Tu, Hailin
 674 Hu, Jie Hu, and Yunhe Wang. Genimage: A million-scale benchmark for detecting ai-generated
 675 image. *Advances in Neural Information Processing Systems*, 36:77771–77782, 2023.
 676

677

A BENCHMARK CONSTRUCTION

A.1 DETAILS ABOUT BENCHMARK CONSTRUCTION

682 **Details about Mask Generation** For partial synthesis models, only part of the image is generated;
 683 therefore, a mask is needed to identify the generated region for evaluating localization methods. We
 684 would like to discuss how this mask is generated in detail. Note that all masks are automatically
 685 generated without any human annotation involved.

686 **IMAGE INPAINTING MODELS** As is discussed, given an image I , we apply SAM on it to achieve
 687 several masks $M = \{m_k\}$, where $m_k = \{(i, j)_k\}$ is a mask. We randomly select a mask $m_{k_0} \in M$,
 688 and use it as the mask to perform image inpainting to generate a new image I' . We then fuse I and
 689 I' following m_{k_0} to achieve the final output synthetic image \hat{I} , which satisfies:
 690

$$\hat{I}_{i,j} = \begin{cases} I_{i,j}, & (i, j) \notin m_{k_0} \\ I'_{i,j}, & (i, j) \in m_{k_0} \end{cases} \quad (1)$$

695 Naturally, the ground truth mask corresponding to \hat{I} is m_{k_0} .
 696

697 **IMAGE EDITING MODELS** An image editing models accept an image I and an editing prompt as
 698 input and produces an edited image I' as output. Naturally, the mask corresponding to the generated
 699 region should be $m_0 = \{(i, j) \mid |I_{i,j} - I'_{i,j}| > 0\}$. However, current image-editing models are not
 700 perfect and may modify regions that should not be edited according to the editing prompt. Therefore,
 701 to achieve a more reasonable editing output and corresponding mask, we first filter regions with
 notable modifications, which is $m_1 = \{(i, j) \mid |I_{i,j} - I'_{i,j}| > \tau\}$, where $\tau > 0$ is a hyperparameter.

702 Note that actually there are multiple channels corresponding to a position (i, j) , so we calculate
 703 $|I_{i,j} - I'_{i,j}| = \sum_c |I_{i,j,c} - I'_{i,j,c}|$, where c is a corresponding channel.
 704

705 Further, we filter out too small regions from m_1 to reduce noise introduced by image editing meth-
 706 ods. Specifically, we first find consecutive regions from m_1 . Each consecutive region is a non-empty
 707 set $m_c \subseteq m_1$ which satisfies $\forall (i, j) \in m_c, (i+1, j) \in m_c \vee (i-1, j) \in m_c \vee (i, j+1) \in m_c \vee (i, j-1) \in m_c$ and $\forall (i, j) \in m_1 - m_c, (i+1, j) \notin m_c \wedge (i-1, j) \notin m_c \wedge (i, j+1) \notin m_c \wedge (i, j-1) \notin m_c$.
 708 As can be seen, $m_1 = m_c^{(1)} \cup \dots \cup m_c^{(n)}$, and $m_c^{(i)} \cap m_c^{(j)} = \emptyset$. We construct the final mask
 709 $m = \bigcup_{i, |m_c^{(i)}| > \gamma} m_c^{(i)}$, where $\gamma > 0$ is a hyperparameter. In this study, we select $\tau = 40$ and
 710 $\gamma = 20$.
 711

712 After achieving this final mask, we apply a similar operation as above by fusing I and I' following
 713 m , which is:
 714

$$\hat{I}_{i,j} = \begin{cases} I_{i,j}, & (i, j) \notin m \\ I'_{i,j}, & (i, j) \in m \end{cases} \quad (2)$$

715 DEEPFAKE METHODS Each deepfake method takes an image I and a face image I_f as input and
 716 produces an image I' as an output. Fortunately, each deepfake method already produces a mask
 717 m indicating the modified region, so there is no need to specifically find the mask. We perform a
 718 similar fusing operation to achieve the final synthetic image \hat{I} :
 719

$$\hat{I}_{i,j} = \begin{cases} I_{i,j}, & (i, j) \notin m \\ I'_{i,j}, & (i, j) \in m \end{cases} \quad (3)$$

720 **Details about Quality Check** For text-to-image, image-to-image, and image inpainting methods,
 721 there is no need to verify the quality of the generated image, as the goal of our benchmark is to faith-
 722 fully reflect the performance of existing image generative models. Manual selection may introduce
 723 additional bias.
 724

725 For image editing and deepfake methods, we sampled several generated images to verify whether
 726 they faithfully follow the instruction (editing instruction or face swapping). Our selected models
 727 generally follow instructions well, therefore we include them to construct our test set.
 728

729 Regarding the mask generation for image editing methods, we select all large consecutive regions
 730 as the edited part without referring to the editing instruction. Our rationale is to best handle the
 731 diversity of editing instruction, including foreground, background, single-object, multiple-object,
 732 style, etc. We believe this design choice best reflects the real performance of current image editing
 733 models.
 734

735 Also, for closed-source models like SeedDream and SeedDream-Edit, since they have too strong
 736 filters, many generated results are marked as unsafe and not responded to, resulting in a relatively
 737 small amount of data belonging to these models. However, the number of images belonging to these
 738 models is still reasonable as indicated in Figure 1.
 739

740 A.2 DETAILS ABOUT PROMPT GENERATION

741 An open-source MLLM (Gemma3-4B) is used to generate image captions (for text-to-image and
 742 image-to-image generation) and image editing instructions (for image editing generation). We pro-
 743 vide prompt details as follows:
 744

745 We manually sampled and checked the generated captions and editing instructions and verified that
 746 they are high-quality. We present examples as follows.
 747

748 A.3 INSIGHTS BEHIND OUR BENCHMARK CONSTRUCTION

749 Just like we have stated in Section 3.1, photo-realism is not a key factor we focus on when construct-
 750 ing our benchmark, and we did not specifically choose samples that appear more indistinguishable
 751

756

757

758

Image Captioning Prompt

759

760

You are a powerful MLLM caption generator.

761

Your task is to describe the content of the given image in detail.

762

You should provide a comprehensive description of the image, including objects, scenery, actions, and any other relevant details.

763

You should also include style, color, lighting if applicable.

764

Do not make any assumptions about the image.

765

If you are unsure about certain aspects of the image, describe only what you can clearly see.

766

Your response should only contain the description without any additional commentary or questions.

767

768

769

Figure 7: Image captioning prompt.

770

771

772

773

774

775

Editing Instruction Generation Prompt

776

777

You are a powerful MLLM image editing prompt generator.

778

Your task is to provide a possible editing instruction based on the given image.

779

You should provide a reasonable editing instruction which prompts modifying the content of the image, such as add, remove or modify some content or style in the image.

780

Your response should only contain the instruction without any additional commentary or questions.

781

782

783

784

Figure 8: Image editing instruction generation prompt.

785

786

787

788

789

Image Captioning Example

790

791

A cartoon-style illustration of a young female character with long, flowing red hair. The hair is styled with a large, swirling curl on the right side of her head and cascades down her back. Her eyes are a dark red color and she has a slight, downward gaze. She is wearing a gray jacket over a dark shirt with a visible, patterned collar. A small, ornate pendant hangs around her neck, featuring a gold-colored bell-shaped element and a small, metallic-looking object. The background is solid white.

792

793

794

795

796

797

798

799

800

801

802

803

Image Editing Instruction Example

804

805

Add a sparkling magical effect to the staff.

806

807

808

809

Figure 9: Image captioning example.

810 to humans because we believe that this may introduce additional bias to our constructed dataset.
 811 Different methods identify and localize synthetic images in different ways, and our goal is to pro-
 812 vide a benchmark faithfully representing the natural distribution of synthetic images to support fair
 813 comparison between different methods.

815 B EXPERIMENT SETUP

817 B.1 METRIC CALCULATION

819 We view the detection task as a binary classification task, which yields four statistics: True Positive
 820 Number (TP), True Negative Number (TN), False Positive Number (FP), and False Negative Number
 821 (FN). The metrics are calculated as:

$$824 \quad Acc = \frac{TP + TN}{TP + TN + FP + FN} \quad (4)$$

$$826 \quad f.Acc = \frac{TP}{TP + FN} \quad (5)$$

$$828 \quad r.Acc = \frac{TN}{TN + FP} \quad (6)$$

831 For mIoU, consider a ground truth mask as $G = \{(i, j)\}$ and a predicted mask as $G' = \{(p, q)\}$, the
 832 mIoU is the average of IoU, which is the average of $\frac{|G \cap G'|}{|G \cup G'|}$. We only calculate mIoU on partial
 833 synthesis images.

836 B.2 CHECKPOINT USAGE

838 As discussed, we did not train any method. Instead, for DeeCLIP, Effort, DRCT, C2P-CLIP, DIRE,
 839 and FIRE, we utilized the pretrained checkpoints from their original paper, and for the remaining
 840 methods, we used checkpoints open-sourced by (Li et al., 2025b) for convenience. Regarding de-
 841 tection&localization methods, we use SIDA-13B, FakeShield-22B, and the open-source HiFi-Net
 842 checkpoints.

843 It is worth noting that these checkpoints may bear slightly different training protocols and datasets
 844 due to the differences in their design and implementation. However, this difference is beyond our
 845 discussion, and the goal of our evaluation is to reveal method performance under a reasonable setup.
 846 If a method is trained using generated images from all models used to construct our benchmark, its
 847 performance will be almost perfect, yet this is not a reasonable scenario. Our evaluation follows a
 848 reasonable and practical evaluation protocol, representing real-world scenarios well.

850 C ADDITIONAL ANALYSIS

852 C.1 DETAILED ANALYSIS OF METHODS

854 We present some additional discussions about the methods evaluated. First of all, we would like to
 855 again note that we did not conduct any training on any specific method. Instead, we use the open-
 856 source trained checkpoints for evaluation. Therefore, if there are some issues during training (e.g.
 857 DIRE (Wang et al., 2023) as suggested by (Cazenavette et al., 2024)), the evaluated result may differ
 858 a lot from the reported values in their original paper. However, we argue that this is exactly the
 859 value of our proposed benchmark - to provide a comprehensive and faithful evaluation of existing
 860 methods.

861 Apart from DIRE (Wang et al., 2023) and FIRE (Chu et al., 2025), most detection-only methods
 862 show superior performance on identifying real images. This observation suggests that identifying
 863 synthetic images is still a giant problem. In contrast, detection&localization methods are bad at both
 real images and synthetic images, indicating a problem in both capabilities.

864 C.2 CASE STUDY: EDITING SCENARIOS
865

866 We present several typical cases to offer a qualitative understanding of existing methods. Specifi-
867 cally, we use SIDA as an example to illustrate the behavior of current detection&localization mod-
868 els. Our analysis focuses on the end-to-end image editing scenario, a context that has been generally
869 overlooked by previous benchmarks.

870 Table 4: Examples of localization results of SIDA on SeedDream Edit.
871

872 Editing 873 Scenario	874 Real Image	875 Edited Image	876 Ground Truth Mask	877 Predicted Mask
878 Add				
880 Modify				
887 Remove				

901 We selected different scenarios and image categories, and the results reveal an interesting trend: cur-
902 rent localization methods tend to predict “foreground distinguishable objects.”, even if the ground
903 truth is sometimes background or not distinguishable objects. This is likely because they are fine-
904 tuned on segmentation models, which are designed for localizing foreground distinguishable objects.
905 As a result, they predict surfboards in the “add” scenario, the person in the “modify” scenario,
906 and the vase in the “remove” scenario. However, editing can occur anywhere, which leads to this bi-
907 ased performance, as shown in Table 4. Therefore, we argue that end-to-end image editing with
908 arbitrary editing prompts provides a practical and challenging scenario for AI-generated image de-
909 tection&localization methods, which should be paid more attention to.
910

911 D USE OF LLMs
912

913 We use LLM to assist writing, including polishing expressions and correcting grammar and word
914 usage. LLM is also used for finding related works. All LLM-generated content is verified by humans
915 before they are included in the manuscript.
916
917